Molecular Crystals and Liquid Crystals

ISSN: 1542-1406 (Print) 1563-5287 (Online) Journal homepage: http://www.tandfonline.com/loi/gmcl20

Electroluminescent properties of diphenylamino-dibenzo[g,p]chrysene derivatives

Dong Young Kim, Young Seok Kim, Hyun Woo Lee, Sujin Jeong, Young Kwan Kim & Seung Soo Yoon

To cite this article: Dong Young Kim, Young Seok Kim, Hyun Woo Lee, Sujin Jeong, Young Kwan Kim & Seung Soo Yoon (2016) Electroluminescent properties of diphenylamino-dibenzo[g,p]chrysene derivatives, Molecular Crystals and Liquid Crystals, 636:1, 99-106, DOI: 10.1080/15421406.2016.1201386

To link to this article: http://dx.doi.org/10.1080/15421406.2016.1201386

Published online: 01 Nov 2016.

MOLECULAR CRYSTALS AND LIQUID CRYSTALS
2016, VOL. 636, 99–106
http://dx.doi.org/10.1080/15421406.2016.1201386

Taylor & Francis
Taylor & Francis Group

Electroluminescent properties of diphenylamino-dibenzo[*g,p*]chrysene derivatives

Dong Young Kim[a], Young Seok Kim[a], Hyun Woo Lee[a], Sujin Jeong[a], Young Kwan Kim[b], and Seung Soo Yoon[a]

[a]Department of Chemistry, Sungkyunkwan University, Suwon, Korea; [b]Department of Information Display, Hongik University, Seoul, Korea

ABSTRACT

We designed and synthesized two diphenylamino-dibenzo[*g,p*]chrysene derivatives. To investigate EL properties of these blue emitting compounds, devices were fabricated as following structure : indium-tin-oxide (ITO) (180 nm) / *N,N′*-di(1-naphthyl)-*N,N′*-diphenyl-(1,1′-biphenyl)−4,4′-diamine (NPB) (50 nm) / 2-methyl-9,10-bis(naphthalen-2-yl)anthracene (mADN); emitters **1** and **2** (3% doping) (20 nm) / tris(8-hydroxyquinolinato)aluminum (Alq_3) (30 nm) / lithium quinolate (Liq) (1 nm) / Al (100 nm). Particularly, a device using 3,6-dimethyl-11,14-bis(diphenylamino)-dibenzo[*g,p*]chrysene as a dopant showed good EL properties with power, luminous, and external quantum efficiency of 0.99 lm/W, 2.28 cd/A, and 2.81%, respectively, at 20 mA/cm^2. The CIE coordinates were (0.15, 0.12) at 6.0 V.

KEYWORDS

Organic light-emitting diode; blue fluorescence; dibenzochrysene; Buchwald–Hartwig reaction

Introduction

Organic light-emitting diodes (OLEDs) have attracted many attentions due to their potential applications in full-color display and solid-state lightning. However, compared to red and green emitters, blue emitters have the poor electroluminescent (EL) performances for the practical applications [1]. Due to their excellent photoluminescent (PL) and EL characteristics, anthracene derivatives have been widely used as emitting materials in OLEDs [2–3]. However, the most anthracene derivatives have also characteristic disadvantages of blue emitters and thus need further to be improved their EL performances.

Thus, many researches have reported the efficient and stable blue light-emitting materials based on various aromatics besides anthracenes [4–7]. Among those examples, dibenzochrysene derivatives are good candidates as blue emitters for OLEDs due to suitable wide band-gap. Also, they have high thermal stabilities and electrochemical properties due to their rigid structures [8]. However, few systematic studies have investigated the EL properties of blue-emitting materials based on dibenzochrysene derivatives.

CONTACT Seung Soo Yoon ssyoon@skku.edu Department of Chemistry, Sungkyunkwan University, 300, Cheoncheon-dong, Jangan-gu, Suwon, Gyeonggi-do, 440-746, Korea; Young Kwan Kim kimyk@hongik.ac.kr Department of Information Display, Hongik University, 72-1, Sangsu-dong, Mapo-gu, Seoul, 121-791 Korea.
Color versions of one or more of the figures in the article can be found online at www.tandfonline.com/gmcl.

Here, we designed and synthesized two diphenylamino-dibenzo[*g,p*]chrysene derivatives; 3,6-dimethyl-11-diphenylamino-dibenzo[*g,p*]chrysene (**1**) and 3,6-dimethyl-11,14-bis(diphenylamino)-dibenzo[*g,p*]chrysene (**2**). These materials (**1** and **2**) have the twisted diphenylamino groups around the extended π-aromatic surfaces of dibenzochrysene. These non-planar structures of materials **1** and **2** disrupt intermolecular interaction and reduce self-aggregation through steric hindrance, and thus would lead to the improved EL performances OLEDs using them as blue emitters [9–10]. Moreover, the effective electron-donating and thus hole-transporting ability of diphenylamine moieties would be expected to have the improved EL properties [5].

Experimental details

Synthesis and characterization

All reactions were performed under nitrogen gas. Solvents were carefully dried and distilled from appropriate drying agents prior to use. Commercially available reagents were used without further purification unless otherwise stated. ^{1}H NMR were recorded on Bruker Avance III 500 MHz NMR spectrometer. Low-resolution mass spectra were measured using a Jeol JMS-AX505WA spectrometer in APCI mode. Elemental analyses (EA) were determined by a Flash 2000 autoanalyzer.

3,6-Dimethyl-11-diphenylamino-dibenzo[*g,p*]chrysene (**1**). 11-Bromo-3,6-dimethyl-dibenzo[*g,p*]chrysene (1.0 mmol) and diphenylamine (1.1 mmol), $Pd_2(dba)_3$ (0.05 mmol), tri-*tert*-butylphosphine (1.0 mmol), sodium *tert*-butoxide (2.0 mmol), toluene (30 ml) were mixed in a flask. The mixture was refluxed at 120°C for 12 h and then the precipitates in reaction mixture were filtered off. The resulting solution was extracted with CH_2Cl_2. The organic layer was washed with water and dried with anhydrous $MgSO_4$. After the evaporation of organic solvents, the crude product was purified by column chromatography using CH_2Cl_2 and recrystallization from CH_2Cl_2/Hex. (yield: 45%). ^{1}H-NMR (500 MHz, $CDCl_3$) [δ ppm]; 8.65 (s, 1H), 8.55 (d, 3H), 8.47 (s, 2H), 8.36 (d, 2H), 7.57 (m, 3H), 7.43 (t, 2H), 7.32 (t, 6H), 7.09 (m, 4H), 2.65 (s, 6H); APCI-MS (*m/z*): 524 [M^++1]; calcd for $C_{40}H_{29}N$: C, 91.74; H, 5.58; N, 2.67. Found: C, 91.53; H, 5.52; N, 2.65.

3,6-Dimethyl-11,14-bis(diphenylamino)-dibenzo[*g,p*]chrysene (**2**). 11,14-Dibromo-3,6-dimethyl-dibenzo[*g,p*]chrysene (1.0 mmol) and diphenylamine (2.2 mmol), $Pd_2(dba)_3$ (0.08 mmol), tri-*tert*-butylphosphine (1.0 mmol), sodium *tert*-butoxide (2.0 mmol), toluene (30 ml) were used and followed the procedure of the synthesis of (**1**). (yield: 75%). ^{1}H-NMR (500 MHz, $CDCl_3$) [δ ppm]; 8.50 (s, 2H), 8.45 (d, 2H), 7.90 (m, 2H), 7.41 (d, 2H), 7.31 (dd, 2H), 7.24 (d, 8H), 7.15 (d, 8H), 7.04 (t, 6H), 2.64 (s, 6H); APCI-MS (*m/z*): 691 [M^++1]; calcd for $C_{52}H_{38}N_2$: C, 90.40; H, 5.54; N, 4.05. Found: C, 90.31; H, 5.48; N, 4.01.

Physical measurements

The UV–Vis absorption and PL spectra of the newly designed materials were measured in dichloromethane (10^{-5} M) using Shimadzu UV-1650PC and Aminco-Bowman series 2 luminescence spectrometers. The fluorescence quantum yields of the emitting materials were determined in dichloromethane at 293 K against 9,10-diphenylanthracene (DPA) as a reference ($\Phi_{DPA} = 0.90$) [13]. The highest occupied molecular orbital (HOMO) energy levels were measured with a low-energy photoelectron spectrometer (Riken-Keiki, AC-2). The energy

band gaps were determined from the intersection of the absorption and PL spectra. The lowest unoccupied molecular orbital (LUMO) energy levels were calculated by adding the corresponding optical band gap energies from the HOMO energy values.

OLED fabrication and measurements

For fabricating OLEDs, indium-tin-oxide (ITO) thin films coated on glass substrates were used, which was 30 Ω / square of the sheet resistivity, and 180 nm of thickness. The ITO-coated glass was cleaned in an ultrasonic bath by the following sequence: acetone, methyl alcohol, distilled water, and stored in isopropyl alcohol for 48 h and dried by a N_2 gas gun. The substrates were treated by O_2 plasma under 2.0×10^{-2} torr at 125 W for 2 min. All organic materials and metals were deposited under high vacuum (5×10^{-7} torr). The devices were fabricated in the following sequence: indium-tin-oxide (ITO) (180 nm) / *N,N′*-di(1-naphthyl)-*N,N′*-diphenyl-(1,1′-biphenyl)-4,4′-diamine (NPB) (50 nm) / 2-methyl-9,10-bis(naphthalen-2-yl)anthracene (mADN); emitters **1** and **2** (3% doping) (20 nm) / tris(8-hydroxyquinolinato)aluminum (Alq_3) (30 nm) / lithium quinolate (Liq) (2 nm) / Al (100 nm), NPB as the hole-transporting layer, mADN as host in the emitting layer, Alq_3 as the electron-transporting layer, and Liq:Al as the composite cathode. The current density (*J*), luminance (*L*), luminous efficiency (LE), power efficiency (PE), external quantum efficiency (EQE), and CIE chromaticity coordinates of the devices were measured with a Keithley 2400, Chroma meter CS-1000A. Electroluminance was measured using a Roper Scientific Pro 300i.

Results and discussion

Scheme 1 shows chemical structures and synthetic scheme of materials **1** and **2**. Compound **1** and **2** were synthesized by Buchwald–Hartwig reactions between diphenylamine and the corresponding arylbromide [11] with the moderate yields (45 and 75%).

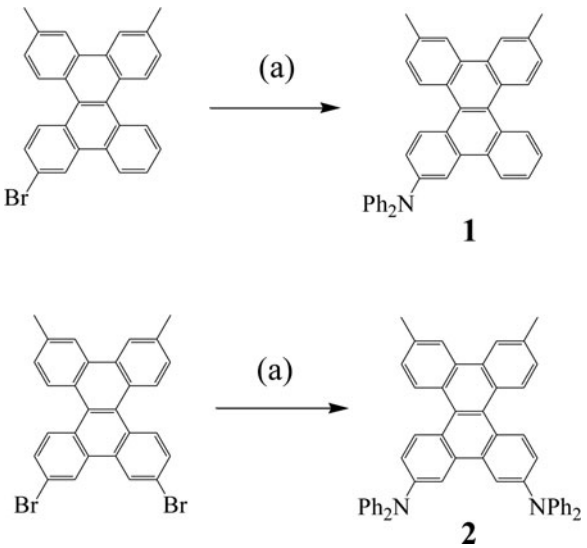

Scheme 1. Structures and synthetic routes of compounds (**1** and **2**).(a) Diphenylamine, $Pd_2(dba)_3$, $P(t\text{-}Bu)_3$, NaOt-Bu, toluene, reflux, 120°C, 12 h.

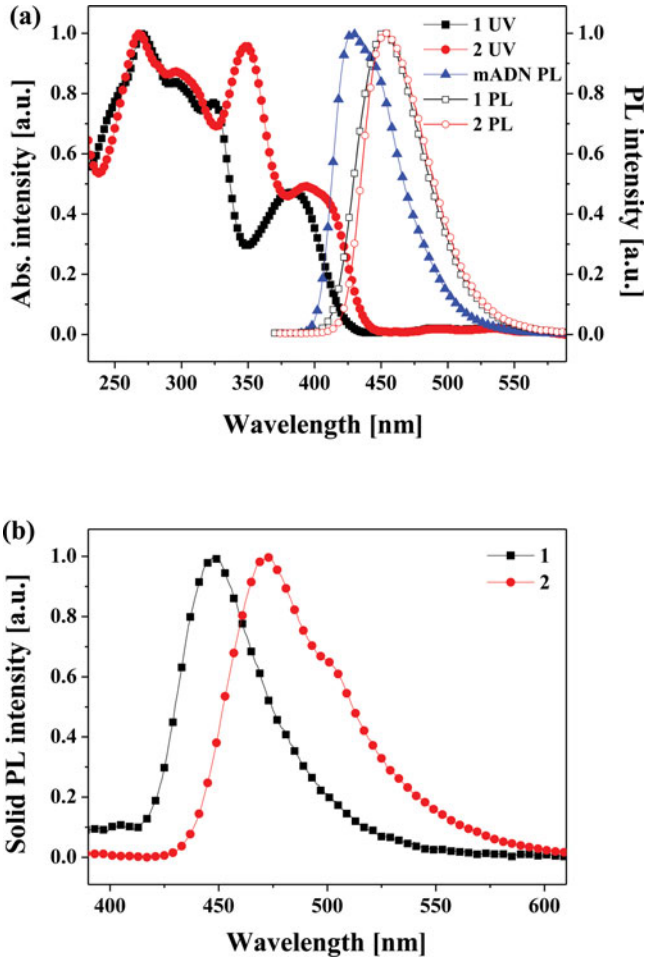

Figure 1. (a) UV–Vis absorption and PL spectra in CH_2Cl_2 (10^{-5} M), and (b) PL spectra in thin film of blue materials (**1** and **2**).

Figure 1 shows the UV–Vis absorption and PL spectra of materials **1** and **2** both in CH_2Cl_2 and thin film state. Their photophysical data are listed in Table 1. In the PL spectra in CH_2Cl_2, the two compounds show similar maximum wavelengths (λ_{max}) of 451 and 454 nm, respectively, in the blue region of the visible spectrum. The maximum emission peak (λ_{max}) of **2** in thin film states show red-shift to 472 nm, due to the molecular packing effect in thin film state [12]. Interestingly, compound **1** shows the almost same maximum emission peaks in

Table 1. Photophysical properties of compounds **1** and **2**.

Compound	UV_{max} [a] [nm]	PL_{max} [a] [nm]	FWHM[a] [nm]	PL_{max} [b] [nm]	HOMO / LUMO[c] [eV]	E_g [d] [eV]	Φ[e]
1	271, 322, 381	451	57	448	−5.42 / −2.39	3.03	0.38
2	269, 296, 393	454	55	472	−5.26 / −2.31	2.95	0.27

[a] CH_2Cl_2 solution (10^{-5} M).
[b] Measured in the film.
[c] The HOMO energy level was determined using a low-energy photoelectron spectrometer (Riken-Keiki, AC-2). LUMO = HOMO + ΔE.
[d] E_g is the energy band gap estimated from the intersection of the absorption and photoluminescence spectra.
[e] Using DPA as a standard; $\lambda_{ex} = 360$ nm ($\Phi_f = 0.90$ in CH_2Cl_2).

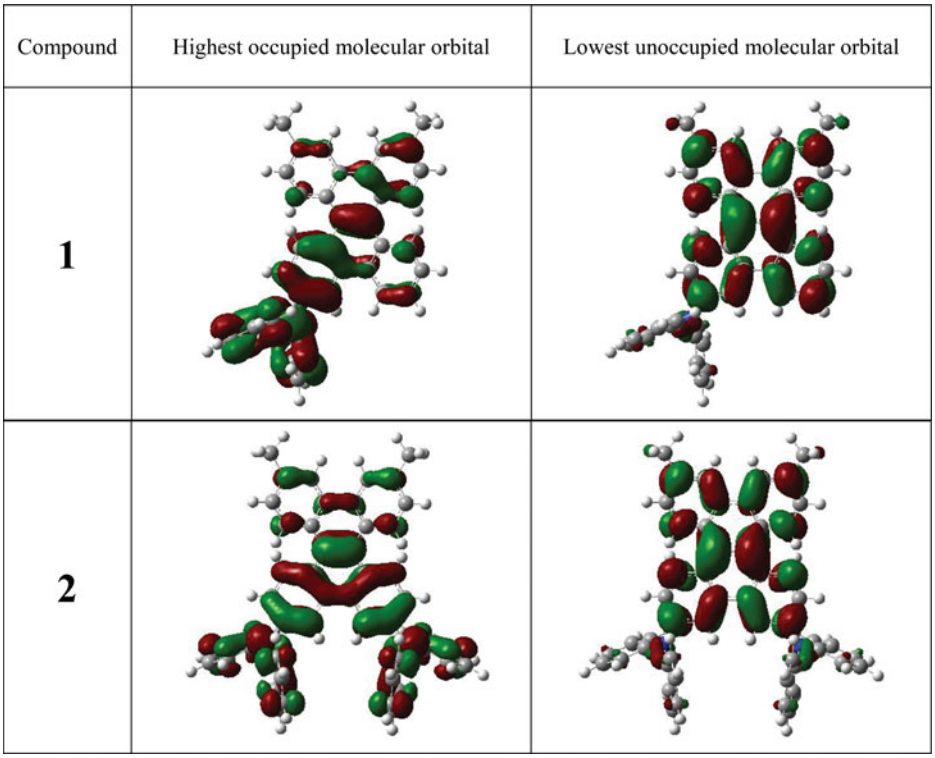

Figure 2. Frontier molecular orbitals of compounds **1** and **2** by using DFT calculation.

solution and solid-state PL spectra (451 and 448 nm), because of the unexpected weak tendency of self-aggregation in compound **1**. In addition, compound **2** exhibits the slightly lower quantum yield than compound **1** in CH_2Cl_2, due to the effective intermolecular interaction.

The HOMO levels of the materials were measured by a low-energy photo-electron spectrometer (Riken-Keiki AC-2) and the LUMO levels were calculated by adding the corresponding E_g from the HOMO values, respectively. The HOMO levels of **1** and **2** are −5.42 and −5.26 eV and the calculated E_g values for them were and 3.03 and 2.95 eV, respectively. The LUMO energy levels of them by adding the E_g from the HOMO energy levels were −2.39 and −2.31 eV, respectively.

To study the observed photophysical properties of compounds **1** and **2** at the molecular level, density functional theory (DFT) calculations of **1** and **2** were carried out by the Becke's three parameterized Lee–Yang–Parr (B3LYP) functional with 6-31G∗basis sets using a suite of Gaussian programs. Figure 2 represents the optimized geometry and electron clouds of HOMO and LUMO of **1** and **2**. In the electron clouds of HOMOs, electrons are spread dibenzochrysene core over the diphenylamine units in both of **1** and **2**. In contrast, electrons are spread only dibenzochrysene cores in both of **1** and **2**, in the electron clouds of LUMO.

To research the EL performances of them as emitting materials in electronic devices, devices were fabricated with the following sequence: ITO (180 nm) / NPB (50 nm) / mADN; emitters **1** and **2** (3% doping) (20 nm) / Alq_3 (30 nm) / Liq (1 nm) / Al (100 nm), (Devices **A** and **B**). In the Figure 3, there are HOMO/LUMO energy-level diagram of the materials used in devices **A** and **B**. The EL spectra of the devices are shown in Figure 4 and their EL properties are summarized in Table 2. The trend of the EL spectra of devices **A** and **B** is similar with the PL spectra of compounds **1** and **2**, which were used as dopants in the corresponding

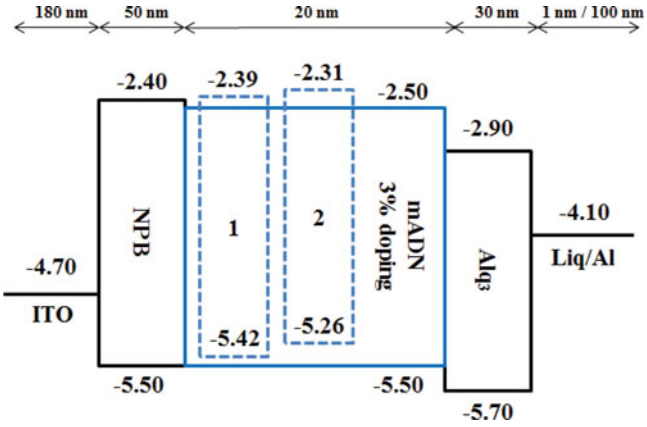

Figure 3. Energy level diagram of the materials used in devices **A** and **B**.

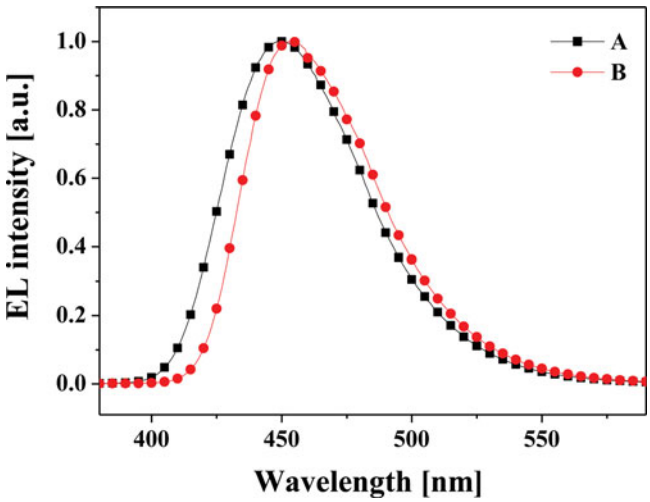

Figure 4. EL spectra of devices **A** and **B**.

devices **A** and **B**. This suggests that EL spectra of devices **A** and **B** were originated from the singlet excited state of each corresponding dopants **1** and **2**. Both devices **A** and B shows deep blue emission with λ_{max} values of 451 and 453 nm in EL spectra and CIE coordinates of (0.15, 0.11) and (0.15, 0.12) at 6.0 V.

Figure 5 illustrates the *J*–*V*–*L* characteristics of devices **A** and **B**. Figure 6 shows luminous efficiency (LE), power efficiency (PE), and external quantum efficiency (EQE) values of devices **A** and **B**, respectively. Especially, device **B** shows the better EL efficiencies than device

Table 2. EL properties of devices **A** and **B**.

Device	λ_{max} [nm]	J [a] [mA/cm^2]	L [a] [cd/m^2]	LE [b/c] [cd/A]	PE [b/c] [lm/W]	EQE [b/c] [%]	CIE [d] (x, y)
A	451	4.0	55	1.67 / 1.65	0.72 / 0.70	2.25 / 2.23	(0.15, 0.11)
B	453	5.9	122	2.29 / 2.28	1.08 / 0.99	2.82 / 2.81	(0.15, 0.12)

[a] Current density and Luminance at 6.0 V.
[b] Maximum values.
[c] At 20 mA/cm^2.
[d] Commission Internationale d'Éclairage (CIE) at 6.0 V.

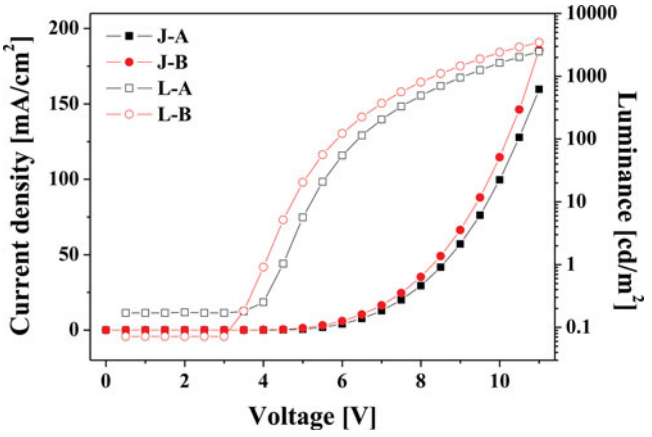

Figure 5. Current density–Voltage–Luminance (*J–V–L*) curves of devices **A** and **B**.

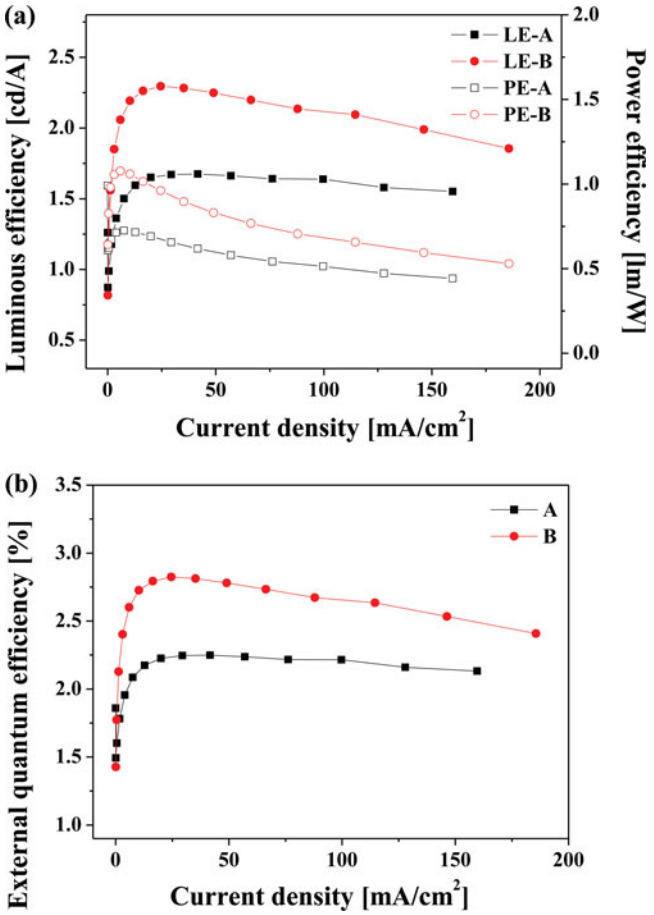

Figure 6. (a) Luminous efficiencies and power efficiencies, and (b) external quantum efficiencies as a function of current density for devices **A** and **B**.

A. As shown in the figure 1(a), the emission spectrum of mADN host of devices **A** and **B** is more effectively overlapped with the absorption spectrum of dopant **2** in device **B** than that of dopant **1** in device **A**. These observations suggest that the Förster energy transfer between host and dopant is more effective in the emitting layer of device **B** than device **A**. The effective energy transfer would contribute to the improved EL efficiencies of device **B** in comparison with device **A**. Intriguingly, the HOMO energy level of dopant **2** (−5.26 eV) in device **B** is higher than that of dopant **1** (−5.42 eV) in device **A**. Therefore, the direct hole trapping into dopant in the emitting layer become more effective in device **B** than device **A**. Presumably, the effective direct hole-trapping would play a partial role in the improved EL efficiencies of device **B** in comparison with device **A**.

Conclusion

In this work, we have synthesized blue fluorescent materials **1** and **2** based on dibenzochrysene emitting core containing diphenylamine groups by Buchwald–Hartwig reactions. Their EL properties were investigated by fabrication of multilayered OLEDs. Especially, a device using material **2** as an emitting material exhibited the deep-blue emission with CIE (x, y) coordinates of (0.15, 0.12) at 6.0 V. This device has the LE, PE, and EQE values of 2.28 cd/A, 0.99 lm/W, and 2.81% at 20 mA/cm^2, respectively. This study shows that dibenzo[*g,p*]chrysene derivatives have the excellent properties as the blue emitting materials for OLEDs.

Acknowledgment

This research was supported by the Samsung Display and Basic Science Research Program through the NRF funded by the Ministry of Education, Science and Technology, South Korea (NRF-2013R1A1A2A10008105).

References

[1] Lee, K. H., Kang, L. K., Lee, J. Y., Kang, S. W., Jeon, S. O., Yook, K. S., Lee, J. Y., & Yoon, S. S. (2010). *Adv. Funct. Mater.*, *20*, 1345.
[2] Wee, K. R., Han, W. S., Kim, J. E., Kim, A. L., Kwon, S. N., & Kang, S. O. (2011). *J. Mater. Chem.*, *21*, 1115.
[3] Zhuang, S., Shangguan, R., Huang, H., Tu, G., Wang, L., & Zhu, X. (2014). *Dyes Pigments.*, *101*, 93.
[4] Tong, Q. X., Lai, S. L., Lo, M. F., Chan, M. Y., Ng, T. W., Lee, S. T., Tao, S. L., & Lee, C. S. (2012). *Synth. Met.*, *162*, 415.
[5] Lee, K. H., Kim, S. O., You, J. N., Kang, S. W., Lee, J. Y., Yook, K. S., Jeon, S. O., Lee, J. Y., & Yoon, S. S. (2012). *J. Mater. Chem.*, *22*, 5145.
[6] Wee, K. R., Ahn, H. C., Son, H. J., Han, W. S., Kim, J. E., Cho, D. W., & Kang, S. O. (2009). *J. Org. Chem.*, *74*, 8472.
[7] Yamaguchi, S., & Swager, T. M. (2001). *J. Am. Chem. Soc.*, *123*, 12087.
[8] Chung, Y. H., Sheng, L., Xing, X., Zheng, L., Bian, M, Chen, Z., & Gong, Q. (2015). *J. Mater. Chem. C.*, *3*, 1794.
[9] Park, H. T., Lee, J. H., Kang, I., Chu, H. Y., Lee, J. I., Kwon, S. K., & Kim, Y. H. (2012). *J. Mater. Chem.*, *22*, 2695.
[10] Lee, H. W., Kim, H. J., Kim, Y. S, Kim, J., Lee, S. E., Lee, H. W., Kim Y. K., & Yoon, S. S. (2015). *J. Lumin.*, *165*, 99.
[11] Hartwig, J. F. (1998). *Angew. Chem. Int. Ed.*, *110*, 2154.
[12] Kim, S. O., Lee, K. H., Kim, G. Y., Seo, J. H., Kim, Y. K., & Yoon, S. S. (2010). *Synth. Met.*, *160*, 1259.
[13] Wu, C. L., Chang, C. H., Chang, Y. T., Chen, C. T., Chen, C. T., & Su, C. J. (2014). *J. Mater. Chem., C.*, *2*, 7188.